STUDIES ON BONDING PROPERTIES BETWEEN POLYPROPYLENE WATERPROOF PLATE AND CONCRETE SEGMENT IN SHIELD TUNNELS

SJ YIN[1*] and M ZHOU[1**]

[1]Key Laboratory for Old Bridge Detection and Reinforcement Technology of Ministry of Transportation, Chang'an University, Xi'an 710064, China; Tel: 86-029-82334868
Email: *yinshujun0505@163.com; **zhoumi@chd.edu.cn

ABSTRACT

This paper studies the threaded polypropylene bar as the connecting piece to line the polypropylene waterproof plate inside concrete segment. The polypropylene bars are welded to the polypropylene waterproof plate so that the polypropylene waterproof plate and the concrete segment can be cast together to achieve high-efficient waterproofing. The bonding properties between polypropylene bar and concrete have been tested. A pull-out test including 16 pull-out specimens composed of concrete cube block and polypropylene bar was conducted under pull-out loading. The parameters included surface type and diameter of polypropylene bar and concrete strength grade. Test results show that the maximum bond strength between polypropylene bar with threads on the surface and concrete reaches 3.14MPa, which is 12.8 times stronger than polypropylene bar with smooth surface. The bond strength between polypropylene bars with a diameter of 30mm has doubled strength than polypropylene bars with a diameter of 25mm. The concrete strength has no significant effect on the bond strength. 3D model of pull-out specimens was established in simulation software ABAQUS. The bonding connection was performed by utilizing the non-linear spring elements. The results display that the stress distributed on concrete starts to radiate from the bonding interface to the surroundings in a dumbbell shape and gradually decreases. The stress distribution on polypropylene bar gradually decreases from the loaded end to the free end. The deviation between calculated value and test value within anchoring range 14%. The finite element model can closely reflect bond-slip characteristics between polypropylene bar and concrete.

Keywords: Plastic waterproof plate, Polypropylene bar, Bonding slip, Pull-out test, Simulation, Non-linear simulating analysis.

1. INTRODUCTION

At present, the shield tunnel segment is mainly self-waterproof, supplemented by the construction of coil or coating waterproof layer. However, the laying or painting process of coil or waterproof coating is complicated and it is easy to be damaged in the process of tying steel bars, which can result in poor durability. Correspondingly, the application of plastic waterproofing materials such as EPO, HDPE and EVA which are fixed with nails or without nails and spliced by cold bonding or hot welding was proposed. It turns out that these three plastic waterproofing boards are all able to effectively reduce the risk of puncture and tear damage to waterproof layer in which the comprehensive test data on EPO is the best (Chen et al., 2021). Li wei (2020) explored the waterproofing system combined self-waterproofing concrete with EVA plastic waterproofing board and found that the waterproof issues of underground station can be coped with effectively through this

system. Zhang Yong et al. (2013) analyzed the waterproof design of joints between adjacent shield tunnel segments and put forward rubber elastic gasket with three different sectional forms. Experimental results revealed that it is reliable to utilize the corresponding rubber elastic gaskets at the joint between adjacent segments to achieve ideal sealing effect. On this basis, Zhang Meicong (2019) proposed to add a water-swelling gasket to the inner side of the gasket set on the outer side of the joint between adjacent shield tunnel segments. The results showed that it can produce better waterproof effect. However, the fixing method of the above-mentioned plastic waterproof board with nails is easy to damage the plastic waterproof board due to insufficient thickness of board and unsecured connection, but without nails cannot guarantee the waterproof quality and service life. Hence, the waterproof scheme which utilizes threaded polypropylene (PP) rods as connectors to line the polypropylene waterproofing board inside concrete segment was proposed, as shown in Figure 1. Due to the manufacturable characteristics and appropriate mechanical property of polypropylene, a high-quality waterproof system can be established by welding the polypropylene rods to polypropylene board and casting them with concrete segment together. Meanwhile, the further exploration of the mechanical performance of the connection between waterproof board and concrete segment is critical, which can provide rationale for further determination of design parameters of the waterproof system.

2.   EXPERIMENTAL INVESTIGATION

2.1   Design of Specimen

To investigate the bonding properties between PP rod and concrete, the central pull-out test was designed and carried out (Song, 1987). The loading end of the PP rod is 330mm away from the loading end surface of the concrete. The free end of the PP rod is 20mm away from the free end of the concrete which is equipped with a displacement gauge. To limit stress concentration at both ends of the concrete, the PVC tube is utilized to segregate the PP rods and concrete at both ends (as shown in Figure 2). The length of PVC tube at each end is settled corresponding to the anchorage length of the PP rod (Xu, 1988a). The parameters included surface type and diameter of polypropylene rod and concrete strength grade (Xu, 1988b). To ensure the effectiveness and reliability of the test data, 4 copies of each type specimen were assembled, a total of 16 specimen, as shown in Table 1.
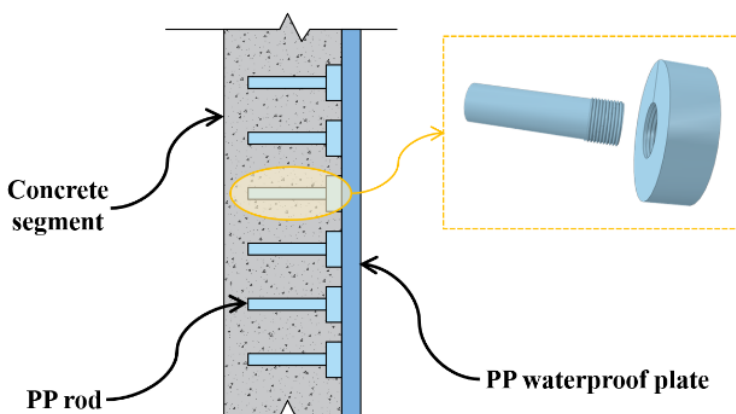

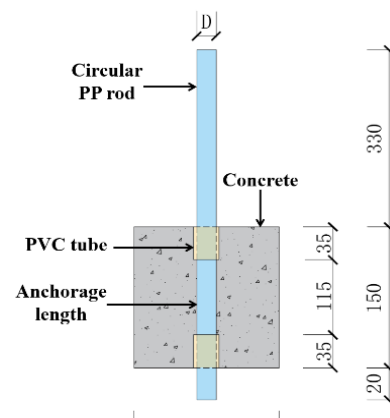**Figure 1: Connection scheme between PP and concrete**

**Figure 2: Diagram of the baseline specimen**

Table 1: Summary of the design types of pull-out specimens

| Specimen number	Surface type of PP rod	Diameter of PP rod （mm）	Concrete strength
PC-G-30-C35	Smooth	30	C35
PC-L-30-C35	Threaded	30	
PC-L-30-C55		30	C55
PC-L-25-C55		25	

Note 1: PC represents polypropylene-concrete pull-out specimens, where P represents polypropylene and C represents concrete; G stands for the smooth surface of PP rod, and L represents the threaded surface of PP rod; The number after the second "-" represents the PP rod diameter, and the character after the third "-" represents the concrete strength grade; For example, PC-L-25-C55 represents a polypropylene-concrete pull-out specimen consisting of a threaded PP rod with 25mm diameter and concrete with a strength of C55.

2.2   Measurement Scheme and Loading Mode

To investigate the distribution law of bonding stress during pull-out process, four strain gauges are evenly arranged inside the PP rod longitudinally within the anchorage length (Nilson, 1971), as shown in Figure 3. Strain which is produced during the pull-out process was measured by a static strain test system DH3816N. The anti-pulling bearing capacity is collected by tensile sensor positioned inside the test machine and automatically output through computer terminal until the specimen is damaged. After the fixation of the specimen, a displacement gauge was placed vertically at the free end of the PP rod.
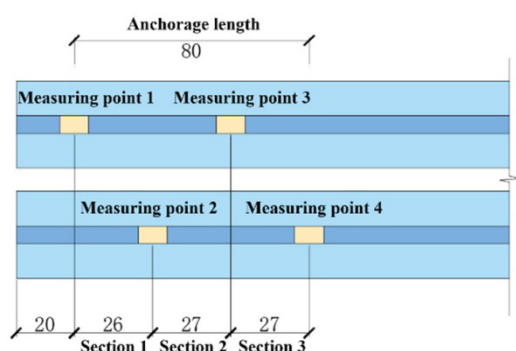
Figure 3: Diagram of strain gauge measuring point and section layout
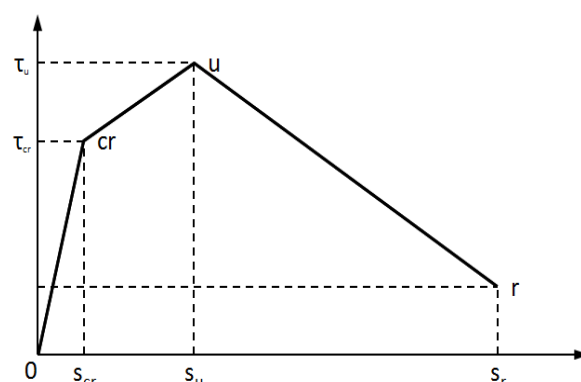
Figure 4: Bonding stress-slip curve between concrete and PP rod

3.   EXPERIMENTAL RESULTS AND DISCUSSION

3.1   Failure Form and Bonding Stress-Slip Relation

Two types of damage occurred in the experiment: the PP rod was pulled out or the PP rod was broken. When the implemented load is greater than the ultimate bonding stress between the PP rod and the concrete, the PP rod will be slowly pulled out from concrete. When the implemented load is less than the ultimate bonding stress between the PP rod and the concrete but greater than ultimate tensile stress of PP, the PP rod will break in the concrete. Due to the much less elastic modulus of PP than concrete, there will be no failure form of concrete rupture. The damage type of specimen and calculated results of bonding strength are summarized as shown in Table 2.

Table 2: Average bonding strength and the summary of failure forms

Specimen Type	Ultimate Load/kN	Ultimate Bonding Strength /MPa	Failure Form
G-30-C35	2.04	0.27	Pull out
L-30-C35	25.99	3.45	Pull out or fracture
L-30-C55	25.70	3.41	Fracture
L-25-C55	13.19	1.75	Fracture

Average bonding stress which can stand for the bonding performance between PP rod and concrete is calculated according to the following equation (1).

$$\tau = \frac{F}{\pi D l_a} \tag{1}$$

The analysis curve represents that the bonding failure process between PP rod and concrete can be roughly divided into three stages: the elastic stage, the local cracking stage and the descent stage. The bonding stress-slip correlation between concrete and PP rods can be expressed uniformly in the form of curves shown in Figure 4. Parameters of curve feature points can be accessed in Table 3.

Elastic stage : $\quad \tau = k_1 s \qquad 0 \leq s \leq s_{cr}$ $\hfill$ (2)

Local cracking stage : $\quad \tau = \tau_{cr} + k_2(s - s_{cr}) \qquad s_{cr} < s \leq s_u$ $\hfill$ (3)

Descent stage : $\quad \tau = \tau_u + k_3(s - s_u) \qquad s_u < s \leq s_r$ $\hfill$ (4)

Table 3: Parameter values of feature points on bonding stress-slip curve

Feature point	Bond stress (N/mm²)	Relative displacement (mm)
Crack value (cr)	τ_{cr} 0.972 $f_{t,r}$	s_{cr} 0.044 D
Ultimate value (u)	τ_u 1.4 $f_{t,r}$	s_u 0.195 D
Remnant value (r)	τ_r 0.67 $f_{t,r}$	s_r 0.456 D

### 3.2 Effect of Surface Form of PP Rod on Bonding Properties

As shown in Figure 5, adding threads to the surface of a PP rod can significantly increase its bonding stress in concrete compared to the PP rod with smooth surface. In local cracking stage, with the increase of implemented load, the bonding force between threaded PP rod and concrete is mainly provided by interlocking force and friction resistance. However, the PP rod with smooth surface in this stage only can rely on the friction to form a bonding force which is considerably less than the interlocking force, resulting in a form of failure in which the PP rod was pulled out from the concrete. With the same diameter of the PP rod and the same concrete strength, adding a thread to the surface of the PP rod can rise its ultimate bonding strength by 12.8 times.

3.3   Effect of Diameter of PP Rod on Bonding Properties
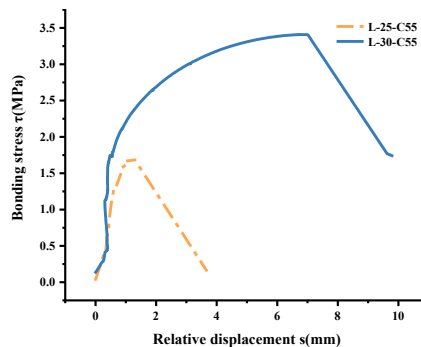
As shown in Figure 6, in the case of the same concrete strength and the same surface type of the PP rod, the ultimate bonding stress increases with the growth of PP rod diameter, as does the ultimate load. Due to larger contact area of the PP rod with larger diameter, the friction and mechanical interlocking force will be greater. The ultimate bonding stress of the PP rod with 30mm diameter in concrete is 94.9% higher than that of the PP rod with 25mm diameter in concrete.

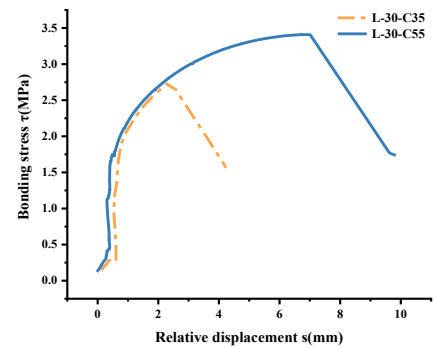### 3.4   Effect of Concrete Strength on Bonding Properties

As observed in Figure 7, the rising stage of the bonding slip curve of the specimen with C35 concrete almost coincides with that of the specimen with C55 concrete. With increasing load, the PP rod in the specimen with C35 concrete is broken early, while the PP rod in the specimen with the C55 concrete still has a certain degree of adhesion with concrete to resist the applied load. Under the same level of load, the high strength concrete has stronger constraints on PP rod which results in a stronger ability to resist the external force, and the relative displacement between the two is less likely to occur which displayed adequate bonding properties. With the same diameter and surface form of PP rod, the ultimate bonding stress of the specimen with C55 concrete is 23.6% higher than that of the specimen with C35 concrete.
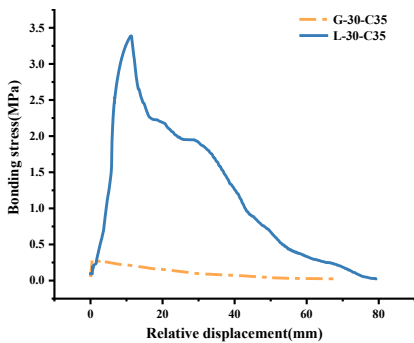
| Figure 5: Different surface forms of PP rod | Figure 6: Different diameters of PP rod | Figure 7: Different concrete strength |

3.5   Distribution Law of Bonding Stress

Under the action of the applied load, the PP rod will produce strain which results in stress. The stress is transmitted to concrete by the bonding performance so that the concrete produces strain, and afterwards the relative displacement between the two is produced. By measuring the strain of PP rod, the bonding stress between PP rod and concrete can be calculated according to the principle of force balance in the micro section of the PP rod. On the assumption that the bonding stress in the micro segment is evenly distributed, it is clear from the equilibrium principle that the tensile difference generated at both ends of the micro-segment is provided by the bonding force generated from the micro-segment surface. Hence, the relationship between the bonding stress and the strain of the PP rod is shown in the following equation (5). Within the anchorage length range, the bonding stress value under each stage load is calculated. This value is numerically integral from the free

end to the loading end, and a cumulative value is finally obtained. This cumulative value should theoretically be equal to the applied load value F of the loading end, as shown in the following equation (6).

$$\tau = \frac{\Delta F}{A} = \frac{A_P \Delta \sigma_P}{sdx} = \frac{A_P(\sigma_{P,i+1} - \sigma_{P,i})}{\pi D h_i} = \frac{DE_P(\varepsilon_{P,i+1} - \varepsilon_{P,i})}{4h_i} \tag{5}$$

$$F = \sum_{i=1}^{n} \tau_i \pi D h_i \tag{6}$$

when the equal sign of equation (6) is not equal, according to the distance of each micro-segment, the difference is assigned to each micro segment according to the inverse symbol law to fine-tune it. The bonding stress values of each micro-segment are connected by a smooth curve, and the variation of the bonding stress with the anchorage position is obtained.

4. FINITE ELEMENT ANALYSIS

The bonding stress-slip relationship between the PP rod and concrete is simulated by nonlinear spring units in finite element analysis software Abaqus/CAE. The bonding stress-slip correlation as mentioned above are endued to spring unites set along anchorage length on PP rod which is simulated by truss unit, as shown in Figure 8. The results display that the stress distributed on concrete starts to radiate from the bonding interface to the surroundings in a dumbbell shape and gradually decreases. The stress distribution on PP rod gradually decreases from the loaded end to the free end, as shown in Figure 9.
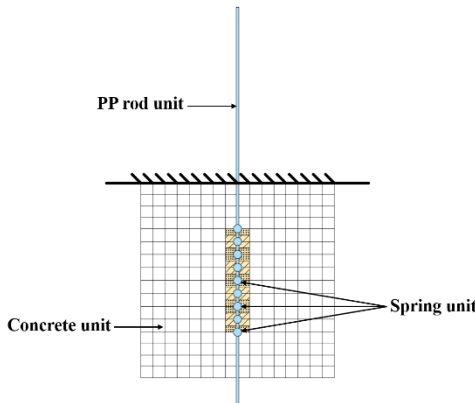

Figure 8: Finite element model of pull-out specimen
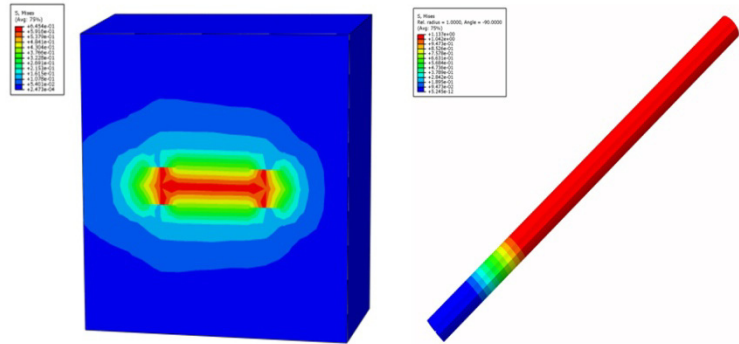
Figure 9: Stress contour plot of concrete and PP rod

As can be seen from Figure 10, 11 and 12, the finite element analysis result is in good agreement with the test result in the initial stage. In this phase, the bonding force between the PP rod and the concrete is greater than that of the external load. As load raises, finite element analysis data and experiment data begin to differ. The difference reached the maximum 14.3% around the peak of bonding stress which remains within an acceptable range. Therefore, it can be known that the results of the finite element analysis obtained by utilizing spring element to simulate the bonding characteristics between the concrete and the PP rod are well consistent with the experimental results, which shows that the finite element model can closely reflect bond-slip characteristics between PP rod and concrete.
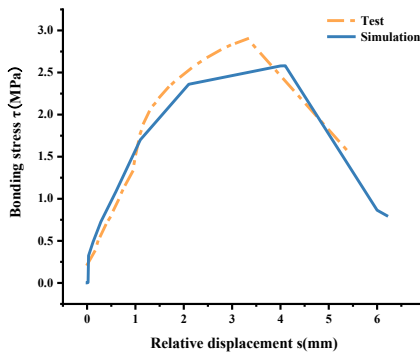
Figure 10: Comparison of testing results and simulation results of PC-L-30-C35
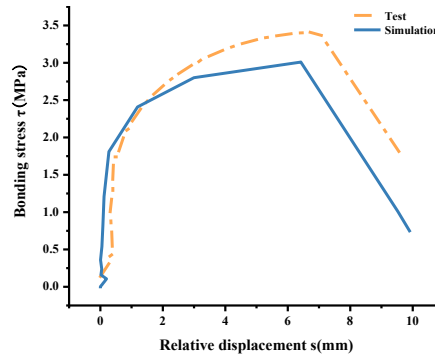
Figure 11: Comparison of testing results and simulation results of PC-L-30-C55
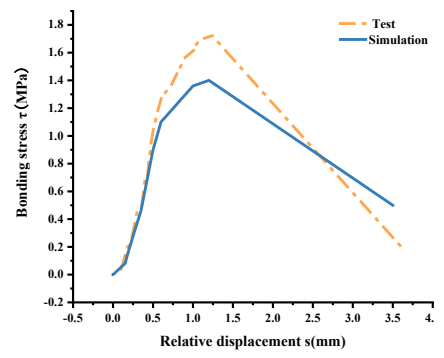
Figure 12: Comparison of testing results and simulation results of PC-L-25-C55

5. CONCLUSIONS

- Two types of damage occurred in the pull-out test: the PP rod was pulled out or the PP rod was broken. The bonding failure process between PP rods and concrete can be roughly divided into three stages: elastic stage, local cracking stage and descent stage.

- With the same concrete strength and the same PP rod diameter, adding threads to PP rod surface or increasing the diameter of PP rod can significantly improve its ultimate bonding stress. In the case of same surface form and same diameter of PP rod, an increasement of concrete strength can improve the ultimate bonding stress to a certain extent, but its influence is less than that of adding thread to the surface of PP rod or increasing the diameter of PP rod.

- Under external pull -out load, the stress distributed on concrete starts to radiate from the bonding interface to the surroundings in a dumbbell shape and gradually decreases. The stress distribution on PP rod gradually decreases from the loaded end to the free end. The maximum deviation between the calculated value and test value within anchoring range reached 14%. The finite element model can closely reflect bond-slip characteristics between PP rod and concrete.

6. DECLARATION OF COMPETING INTEREST

The authors declare that they have no known competing financial interests or personal relationships that could have appeared to influence the work reported in this paper.

7. ACKNOWLEDGEMENTS

8.   REFERENCES

Chen, L, Zheng, XF & Li, L, 2021. Research on the application of EPO waterproof material in rail transit waterproof engineering. *Tunnel and Rail Transit*, S1:176-178.

Li, W, 2020. Metro waterproof construction technology. *China Construction*, 8:96-97.

Nilson, AH, 1971, Bond Stress-slip Relationship in Reinforced Concrete. Report No.345. Department of Structure Engineering, Cornell University, Ithaca, New York.

Song, YP, 1987. Study on Bonding Slip Performance Between Steel Bar and Concrete. *Journal of Dalian Institute of Technology*, 26:93-100.

Xu, Y, Shao, ZM & Shen, W, 1988. Bonding Anchorage Strength of Steel Bars and Concrete. *Architectural Science*, 4:8-14.

Xu, Y, Shen, W & Wang, H, 1994. Experimental Study on Adhesion Anchorage Performance of Reinforced Concrete. *Journal of Architectural Structures*, 15:26-37.

Zhang, MC, 2019. Waterproofing Design for Cross-ocean Shield Tunnel of Xiamen Subway Line 2. *China Building Waterproofing*, S1:24-27.

Zhang, Y & Jia, Y, 2013. Joint Waterproofing Design for River-crossing Shield Tunnel of Nanjing Subway, Line 10. *China Building Waterproofing*, 16:18-25.